INTRAVAL PROJECT

Phase 1 Case 2

RADIONUCLIDE MIGRATION IN SINGLE NATURAL FRACTURES IN GRANITE

NEA

SKi

THE INTERNATIONAL INTRAVAL PROJECT

Phase 1 Case 2

RADIONUCLIDE MIGRATION IN SINGLE NATURAL FRACTURES IN GRANITE

Editor: K. Skagius

NEA SKI

ORGANISATION FOR ECONOMIC CO-OPERATION AND DEVELOPMENT

Pursuant to Article 1 of the Convention signed in Paris on 14th December 1960, and which came into force on 30th September 1961, the Organisation for Economic Co-operation and Development (OECD) shall promote policies designed:

- to achieve the highest sustainable economic growth and employment and a rising standard of living in Member countries, while maintaining financial stability, and thus to contribute to the development of the world economy;
- to contribute to sound economic expansion in Member as well as non-member countries in the process of economic development; and
- to contribute to the expansion of world trade on a multilateral, non-discriminatory basis in accordance with international obligations.

The original Member countries of the OECD are Austria, Belgium,Canada, Denmark, France, Germany, Greece, Iceland, Ireland, Italy, Luxembourg, the Netherlands, Norway, Portugal, Spain, Sweden, Switzerland, Turkey, the United Kingdom and the United States. The following countries became Members subsequently through accession at the dates indicated hereafter: Japan (28th April 1964), Finland (28th January 1969), Australia (7th June 1971) and New Zealand (29th May 1973). The Commission of the European Communities takes part in the work of the OECD (Article 13 of the OECD Convention). Yugoslavia has a special status at OECD (agreement of 28th October 1961).

NUCLEAR ENERGY AGENCY

The OECD Nuclear Energy Agency (NEA) was established on 1st February 1958 under the name of the OEEC European Nuclear Energy Agency. It received its present designation on 20th April 1972, when Japan became its first non-European full Member. NEA membership today consists of all European Member countries of OECD as well as Australia, Canada, Japan and the United States. The Commission of the European Communities takes part in the work of the Agency.

The primary objective of NEA is to promote co-operation among the governments of its participating countries in furthering the development of nuclear power as a safe, environmentally acceptable and economic energy source.

This is achieved by:

- *encouraging harmonization of national regulatory policies and practices, with particular reference to the safety of nuclear installations, protection of man against ionising radiation and preservation of the environment, radioactive waste management, and nuclear third party liability and insurance;*
- *assessing the contribution of nuclear power to the overall energy supply by keeping under review the technical and economic aspects of nuclear power growth and forecasting demand and supply for the different phases of the nuclear fuel cycle;*
- *developing exchanges of scientific and technical information particularly through participation in common services;*
- *setting up international research and development programmes and joint undertakings.*

In these and related tasks, NEA works in close collaboration with the International Atomic Energy Agency in Vienna, with which it has concluded a Co-operation Agreement, as well as with other international organisations in the nuclear field.

Foreword

Currently, radioactive waste management programmes in OECD countries cover a wide range of activities aiming at the gradual implementation of disposal concepts for various types of waste. This concerns, in particular, the institutional and regulatory framework as well as research and development activities. In some countries, site selection and characterisation programmes for high-level waste disposal are at a relatively advanced stage. Several countries already have repositories for low-level waste in operation. Among these activities, safety issues are a common concern, and, therefore, enjoy a high priority in international co-operative programmes.

INTRAVAL is an international project concerned with the use of mathematical models for predicting the potential transport of radioactive substances in the geosphere. Such models are used to help assess the long-term safety of radioactive waste disposal systems. The INTRAVAL project was established to evaluate the validity of these models. Results from a set of selected laboratory and field experiments as well as studies of occurences of radioactive substances in nature (natural analogues) are compared in a systematic way with model predictions. Discrepancies between observations and predictions are discussed and analysed.

Twenty-two organisations from thirteen OECD countries participate in INTRAVAL. The Swedish Nuclear Power Inspectorate (SKI) is the managing participant and the OECD/Nuclear Energy Agency, Her Majesty's Inspectorate of Pollution (HMIP/DOE), United Kingdom, and Kemakta Consultant Co., participate in the Project Secretariat.

INTRAVAL finished its first phase in 1990. Phase 1 of the project was comprised of seventeen test cases, and thirteen of these have been extensively analysed. This report is one in a series of eleven INTRAVAL Technical Reports documenting the results and conclusions of Phase 1. In addition, short descriptions of the experiments behind the test cases are compiled in a separate Technical Report. The integrated results and overall conclusions of INTRAVAL Phase 1 are given in a Summary Report.

A second phase of the INTRAVAL project was initiated in 1990. Phase 2 of the study will conclude the INTRAVAL project in 1994.

Abstract

The INTRAVAL study addresses validation of geosphere transport models for use in repository performance assessment by examining various test cases relevant to radioactive waste disposal. This report describes the results from INTRAVAL test case 2 which is based on a set of laboratory experiments studying migration of non-sorbing as well as sorbing tracers in a single fracture in granitic cores. Three project teams have investigated this test case. Models including advection, dispersion, sorption to the fracture surface, matrix diffusion and sorption within the rock matrix were calibrated against the experimental breakthrough curves. Obtained best-fit values of the parameters determining the interaction between tracer and rock were in fair agreement with independently measured data. Models neglecting matrix diffusion and sorption within the rock matrix gave poor fits to the experimental data. These results suggest the need to include matrix diffusion and matrix sorption in the model to represent data for this test case. Furthermore, it was not possible to distinguish between hydrodynamic dispersion and channelling dispersion since equally good fits were obtained with both models. Equally good fits were also obtained with models assuming constant fracture aperture and variable fracture aperture. In the context of performance assessment of repositories in fractured rock, the major outcome from this test case is additional support for the inclusion of matrix diffusion and matrix sorption in the transport models.

Table of Contents

1. Introduction

Radioactive waste arises as a by-product of nuclear generation of electricity and of the use of radio-isotopes in medicine and industry. Many countries are currently evaluating ways to dispose of radioactive waste safely. It is generally agreed that the preferred option for disposal is to process the waste into stable solid forms and place these in an underground repository in a suitable geological formation. This approach aims to keep the radioactive materials away from Man's immediate environment (the biosphere) until radioactive decay has reduced their radioactivity to an acceptable level.

The natural pathway for radionuclides from radioactive waste buried in an underground repository to return to the biosphere is the groundwater pathway. Flowing groundwater can dissolve radionuclides from the waste and transport them to the biosphere. A well-designed repository will be located to ensure that these dissolution and transport processes are extremely slow. Analysis of the groundwater pathway plays an important role in selecting a suitable site for a potential repository, and in a performance assessment for a repository.

Such analyses must use mathematical models in order to assess the performance of a potential repository over the very long times that must be considered. It is clearly desirable that confidence can be placed in the models used. To this end, computer models must be verified, that is shown accurately to represent the intended mathematical models, which must be validated, that is shown adequately to represent physical phenomena.

Several international collaborative projects have been set up to assist in the verification and validation of models for groundwater flow and transport. The first of these was INTRACOIN [1] which was set up in 1981 to address verification and validation of models for radionuclide transport. INTRACOIN was succeeded by HYDROCOIN [2] which addressed the issues of verification and validation of groundwater flow models. In turn HYDROCOIN was succeeded by INTRAVAL [3,4] which began in 1987. INTRAVAL seeks to address validation of geosphere transport models for use in repository performance assessments.

As in INTRACOIN and HYDROCOIN, effort in INTRAVAL is structured around a number of test cases. The INTRAVAL test cases are designed to examine a range of materials that might be relevant to radioactive waste repositories, and to explore a range of scales from laboratory experiments through field experiments up to natural analogues. The test cases were chosen taking into account the status of the experimental programme, the availability of data, the possibility of interaction between modellers and experimentalists and the relevance to validation issues.

Laboratory experiments have two purposes. They help to develop understanding of physical and chemical processes under well-defined conditions, and they provide data. These two aspects are

not independent because the interpretation of an experiment to provide data depends upon the model used.

The main advantages of laboratory experiments relative to field experiments are that the experimental system can be set up in a well defined manner and characterised much more completely. The experimental conditions can be much more closely controlled and parameters varied. However, there are still often difficulties in carrying out experiments. The main disadvantage of laboratory experiments is that the temporal and spatial scales that can be addressed are much smaller than those considered in safety assessment. Field experiments can examine larger length and time scales than laboratory experiments, although the scales that can be considered are still smaller than the scales considered in performance assessment. The length and time scales of interest in a performance assessment can only be addressed by means of natural analogues, although these cannot be controlled.

This report presents a summary of the work that has been carried out on INTRAVAL test case 2, which is based on laboratory experiments on the migration of tracers in natural fractures in granite cores. The following three Project Teams have contributed results for this test case:

- Japan Atomic Energy Research Institute (JAERI),
- Pacific Northwest Laboratory (PNL) acting for the U.S. Department of Energy,
- Royal Institute of Technology (KTH) acting for the Swedish Nuclear Fuel and Waste Management Co.

The KTH Project Team did their modelling work prior to the start of the INTRAVAL project, in connection to the experimental programme. Documentation of this work was available to all other teams tackling this test case.

2. Experiments

2.1 Purpose

Test case 2 is based on a set of laboratory experiments performed at the Department of Nuclear Chemistry of the Royal Institute of Technology, Stockholm, Sweden [5,6,7,8,9,10]. Tracer dispersion, sorption, matrix diffusion, and channelling effects were studied, and the fracture aperture was determined. Experimental results were used for fitting of models, taking into consideration channelling and hydrodynamic dispersion. Another objective was to estimate to what extent independently measured diffusivities and distribution ratios could be used in modelling and interpretation of tracer migration experiments. These experiments were selected as a test case because of their relevance to the study of fluid flow in natural fractures.

2.2 Overview

Migration experiments were performed in granite cores from the Stripa mine, located in central Sweden. Each core contained a single natural fracture running parallel to the core axis. These experiments were intended to characterize both sorption, and matrix diffusion in such fractures. Background information on core composition, geochemical, geophysical, and geological data can be found in the general reports of the Stripa Project [11,12,13,14].

The experiments were performed using non-sorbing (Na-lignosulphonate, ^{3}H, ^{131}I), moderately sorbing (^{85}Sr and ^{134}Cs), and strongly sorbing tracers (^{152}Eu, ^{235}Np, ^{237}Pu, ^{241}Am, and ^{99}Tc). Artificial groundwater with a tracer was introduced into the fracture at one end of the core, and the tracer breakthrough curve at the other end of the core was monitored. The spatial scales of the experiments were of the order of 20 - 30 cm (moderately sorbing tracers), and 8 - 10 cm (strongly sorbing tracers). The duration of the experiments was from minutes to hours in the case of moderately sorbing tracers, and up to several weeks in the case of strongly sorbing tracers.

When strongly sorbing tracers were used, the tracer distribution inside the core was determined at the end of each experiment.

Complementary sorption experiments with crushed granite, with material from the lining of fractures, as well as on intact fissure surfaces were also performed [6]. Distribution ratios were calculated for ^{85}Sr, ^{134}Cs, and ^{152}Eu. The material used for these experiments was also extracted from the Stripa mine at a similar depth.

2.3 Experimental Design

2.3.1 General

The samples were cylindrical cores of granite from the Stripa mine, taken at a depth of 360 m below ground level. The core surfaces were sealed with a coating of urethane lacquer to prevent water leaving the core at other locations than the end outlet. The coated granite cylinders were mounted between two plexiglas endplates containing shallow inlet and outlet channels slightly wider than the aperture of the fractures. Figure 2.1 shows the experimental setup.

Prior to each experiment, a synthetic ground water (with the composition described in Table 2.1) was pumped through the bore core until equilibrium was established with the fracture surface.

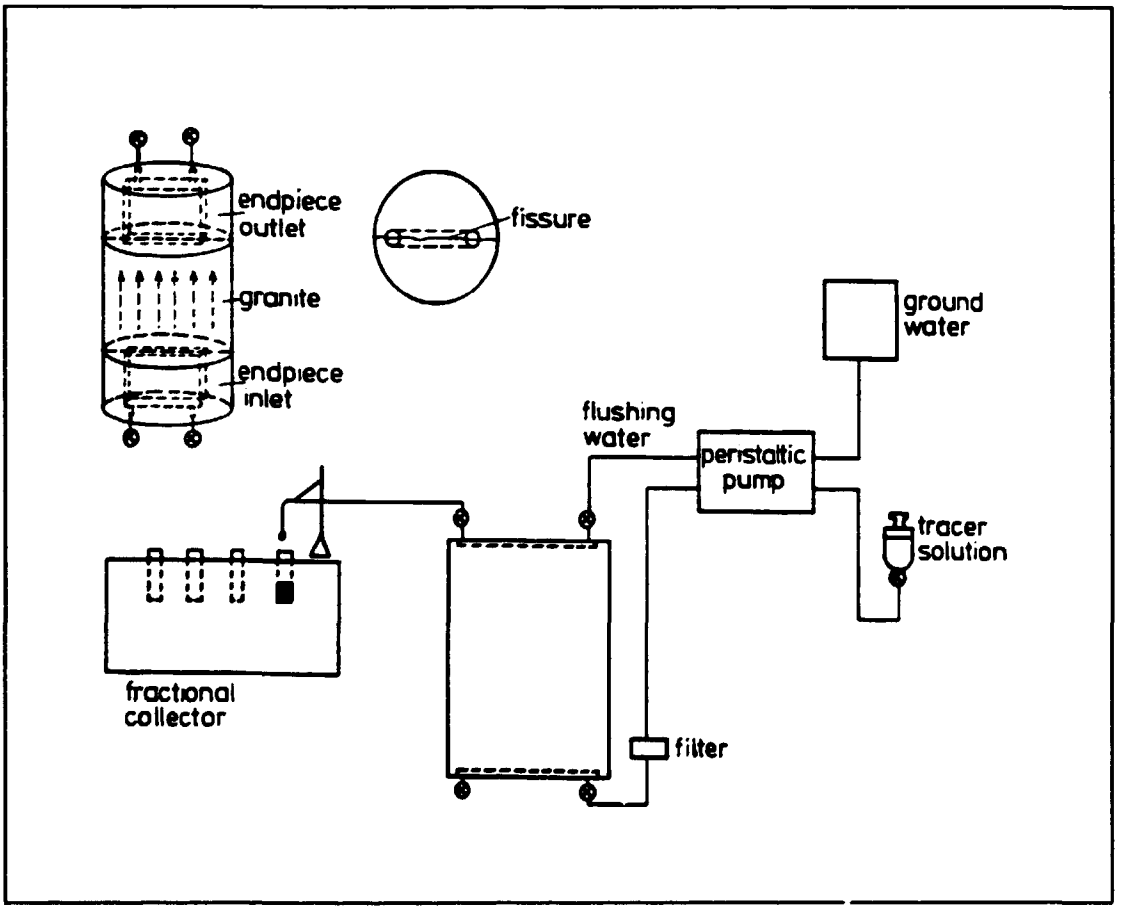

Figure 2.1 Experimental setup.

Table 2.1 Composition of the artificial groundwater

Species	Concentration mole/l	ppm
HCO_3^-	$2.014 \cdot 10^{-3}$	123
$H_4SiO_4^-$	$2.056 \cdot 10^{-4}$	12
SO_4^{2-}	$1.000 \cdot 10^{-4}$	9.6
Cl^-	$1.973 \cdot 10^{-3}$	70
Ca^{2+}	$4.477 \cdot 10^{-4}$	18
Mg^{2+}	$1.774 \cdot 10^{-4}$	4.3
K^+	$1.000 \cdot 10^{-4}$	3.9
Na^+	$2.836 \cdot 10^{-3}$	65
pH	8 - 8.2	
Eh	260 mV	

In the tracer tests artificial groundwater with a tracer was fed into the inlet channel by means of a four-channel peristaltic pump. In the case of low flow rates, flushing water was simultaneously fed by the same pump through the output channel to reduce the time delay due to the channel volume of the end piece (see Figure 2.1). The effluent was continuously fed to a fractional collector for analysis of the tracer concentration.

2.3.2 Moderately Sorbing Tracers

Tests with the non-sorbing lignosulphonate ion LS^- and with ^3H , and the moderately sorbing ions ^{85}Sr and ^{134}Cs were performed in rock sample L (a 30 cm long core with a diameter of 20 cm). Experiments using the non-sorbing tracers ^3H, ^{131}I, ^{82}Br, and the moderately sorbing tracer ^{85}Sr, were performed in rock samples 5 (18 cm long with a diameter of 10 cm) and 6 (27 cm long with a diameter of 10 cm).

The water flow in the fracture was characterised by feeding a solution of a non-sorbing tracer to the inlet channel. The injection flow rates of these tracers were between 0.03 and 0.18 ml/min (sample L) and between 0.22 and 1.62 ml/min (samples 5 and 6). The moderately sorbing tracers were added either by continuous feed, or as a pulse of adequate duration (normally 15 minutes). The flow rates in these tests were between 0.08 and 1.05 ml/min (sample L) and between 0.75 and 1.25 ml/min (samples 5 and 6). After a pulse injection, artificial ground water was pumped through the fissure.

A fraction collector was used to continuously collect the effluent. Based on preliminary experiments, the sampling time was set to be short compared to the rise of the breakthrough curve. When tracer was input as a pulse, the pulse duration was kept short compared to the tracer residence time in the rock sample.

2.3.3 Strongly Sorbing Tracers (Actinides)

The strongly sorbing tracers, ^{152}Eu(III), ^{235}Np(V), ^{237}Pu(IV), ^{241}Am(III), ^{99}Tc(VII), and ^{99}Tc(IV), were used in conjunction with some smaller rock samples (8 to 10.5 cm long with a diameter of 8 cm). Also in these experiments, the flow in the fracture was characterised by injecting the non-sorbing tracer NaLS. The tracers were added as 15 minute pulses in the manner described previously. A steady flow through the fissure of about 0.1 to 0.12 ml/min was used. Artificial ground water was thereafter pumped through the fracture. After several hundred fracture-volumes had passed the fracture, the cores were cracked open and the tracer distribution on the fracture surfaces measured.

2.3.4 Complementary Experiments

Independent sorption experiments on crushed granite and fracture-surface material, using ^{85}Sr, ^{134}Cs, and ^{152}Eu as tracers, were performed on material from a similar location to the bore cores used in the migration experiments [8]. The granite samples were crushed and sorted according to size by wet sieving. The radionuclide solutions were prepared by dilution of acid stock tracer solutions with the same artificial ground water as described in Table 2.1.

To determine the distribution ratios, R_d, 100 mg of crushed and sieved material were brought into contact with 3 cm^3 of ground water in polypropylene tubes and gently agitated. Tracers were added to give concentrations (moles/litre) of $2.5 \cdot 10^{-11}$ for ^{85}Sr, $1.1 \cdot 10^{-9}$ for ^{134}Cs, and $5 \cdot 10^{-8}$ for ^{152}Eu. Activity measuring at regular intervals of time of both the solid phase and the solution, allowed distribution ratios to be determined.

For the sorption on intact rock, a number of 1.2 cm^2 surfaces were sealed off and brought into contact with solutions of radionuclides as shown in Figure 2.2. After 48 hours, the activity on each surface was measured with the NaI detector.

In addition, the cation exchange capacity (CEC) was measured by isotope dilution (^{22}Na as tracer, planar 2x2 inches NaI detector). Samples containing 100 mg of crushed material and 3 cm^3 of a 0.5 mole/litre NaCl spiked with ^{22}Na were brought to equilibrium and vacuumfiltered through a 0.5 µm polypropylene filter. The activity of the solution was then measured with the NaI detector.

2.4 Available Results

2.4.1 Moderately Sorbing Tracers

The migration experiments produced breakthrough curves for each of the tracers used (relative concentration as a function of time). The tracer concentration in the solutions was directly obtained by measuring the optical absorption (lignosulphonate) or by activity counting.

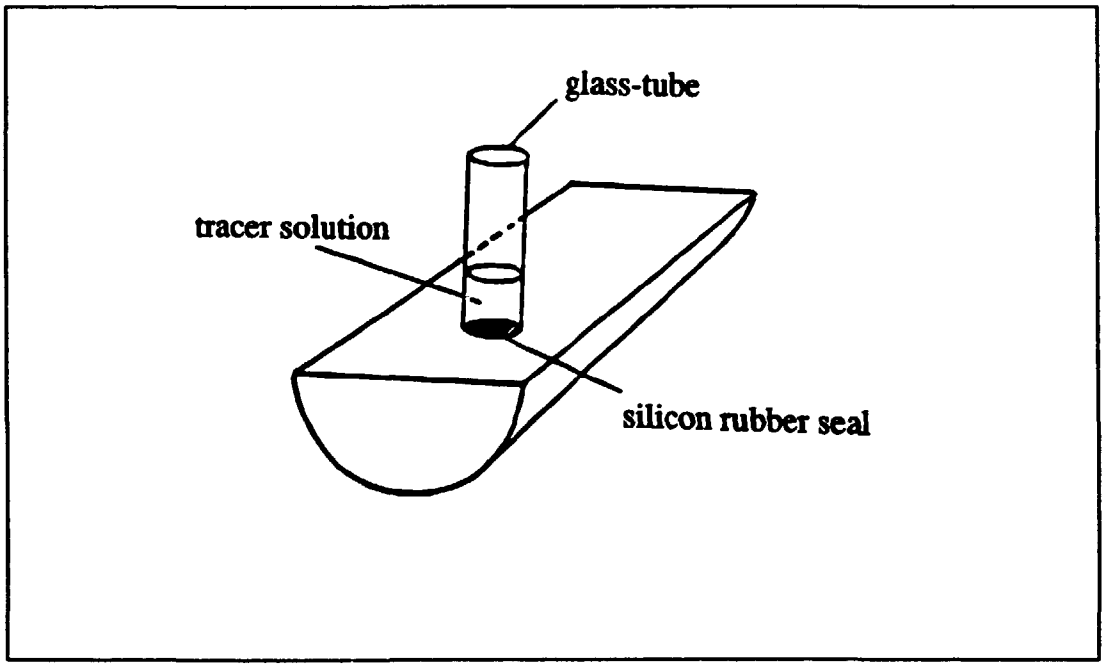

Figure 2.2 Setup for measuring radionuclide sorption on intact fissure surfaces.

Several runs were performed with the non-sorbing and moderately sorbing tracers for each of the three cores described above. The tracers were:

- NaLS, ^{3}H, ^{85}Sr, and ^{134}Cs for core sample L.
- NaLS, ^{3}H, ^{85}Sr, ^{131}I, and $^{82}Br(NH_4Br)$ for sample 5 and 6.

The primary data that were available from each run are:

- sample diameter and length,
- pump-flow and flush-flow,
- tracer concentration of inlet solution,
- standard activity of the inlet solutions,
- optical absorption of the inlet solutions,
- collection time between each sampling,
- activity in outlet solutions as a function of time,
- optical absorption in the outlet solutions as a function of time.

An example of breakthrough curves for the non-sorbing ion LS^- and the moderately sorbing strontium ion in rock core 5 is shown in Figure 2.3. In both runs, the injection flow rate is 1.25 ml/min.

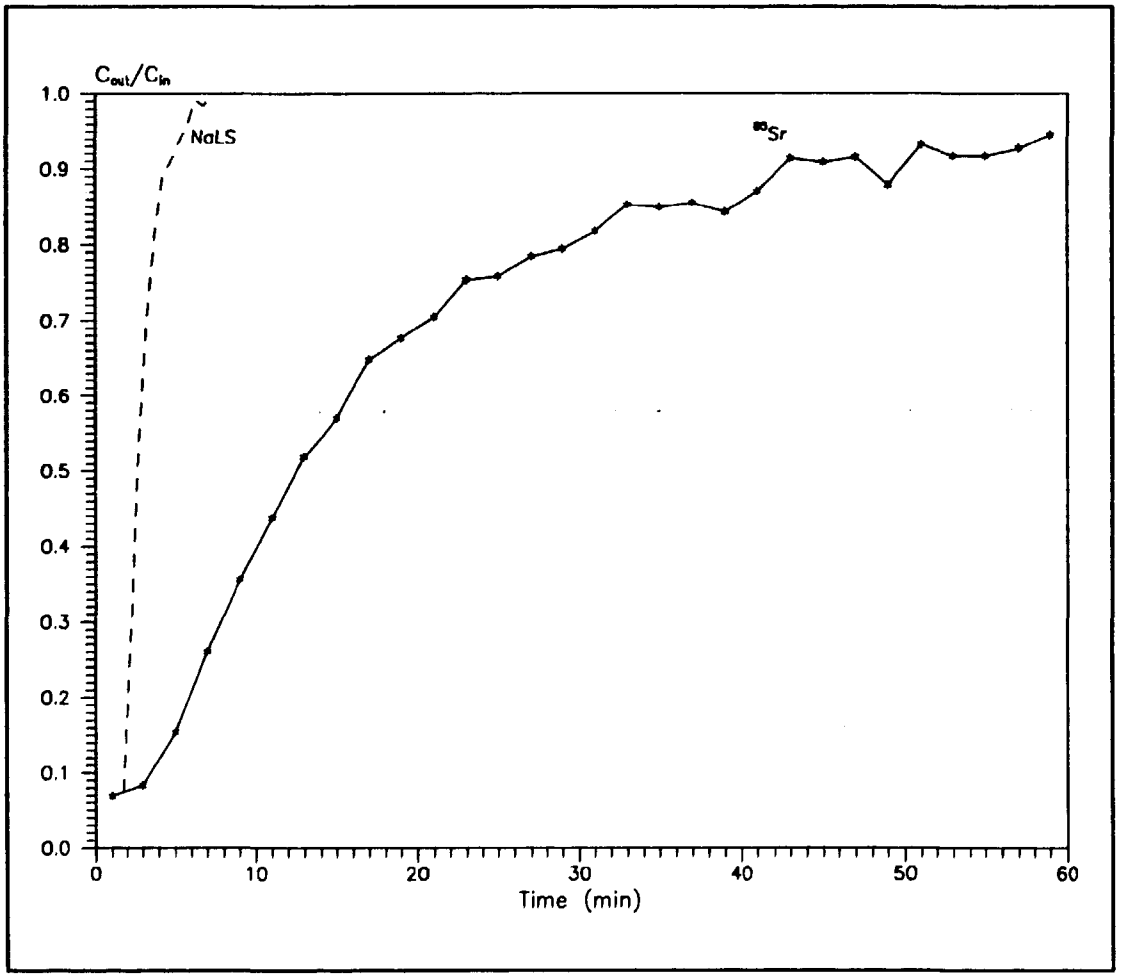

Figure 2.3 Breakthrough curve for the non-sorbing NaLS and the sorbing Sr in rock core 5. Injection flow rate in both runs is 1.25 ml/min.

2.4.2 Strongly Sorbing Tracers

Migration experiments performed with strong sorbing tracers (^{152}Eu(III), ^{235}Np(V), ^{237}Pu(IV), ^{241}Am(III), and ^{99}Tc(IV)) generated effluent concentration versus time curves as well as the radionuclide distribution on the fracture surfaces. Examples of a breakthrough curve and the final distribution of the ^{241}Am tracer on the fracture surface, 122.5 hours after start of tracer injection, are shown in Figure 2.4 and 2.5, respectively. The breakthrough curve corresponds to a tracer pulse of 15 minutes duration and 0.12 ml/min injection flow rate in a 94 mm long core with a diameter of 38 mm. Figure 2.4 also shows the corresponding breakthrough curve for the water flow characterising tracer LS^-.

A small fraction (less than a few percent) of the total activity of ^{152}Eu, ^{235}Np, ^{241}Am, and $^{99m}Tc(IV)$ was transported through the fissure with nearly the same velocity as water (see Figure 2.4). Inserting a 0.21µm filter between the tracer solution reservoir and the inlet channel greatly reduced the fast-moving fraction, clearly indicating that the activity was carried by particulate matter. No fast-moving fraction was observed with ^{237}Pu. The results available are from experiments without the 0.21 µm filter.

The fracture volume, V_f, is also given. It was calculated from the LS^- data using the formula: $V_f = q_w t_w$ where q_w is the water flow (ml/min) and t_w the residence time of LS^- in the fracture (minutes).

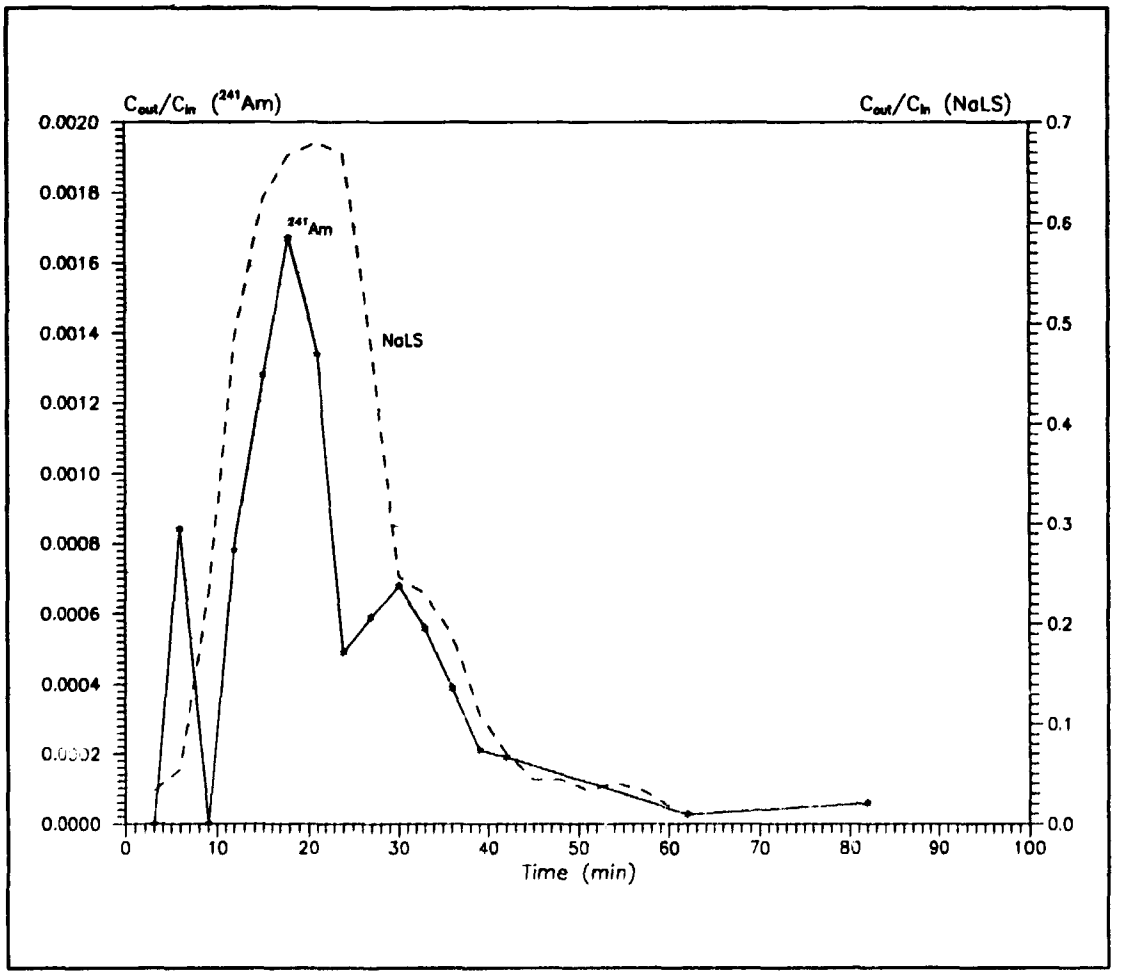

Figure 2.4 Breakthrough curves for the non-sorbing NaLS and the sorbing ^{241}Am.

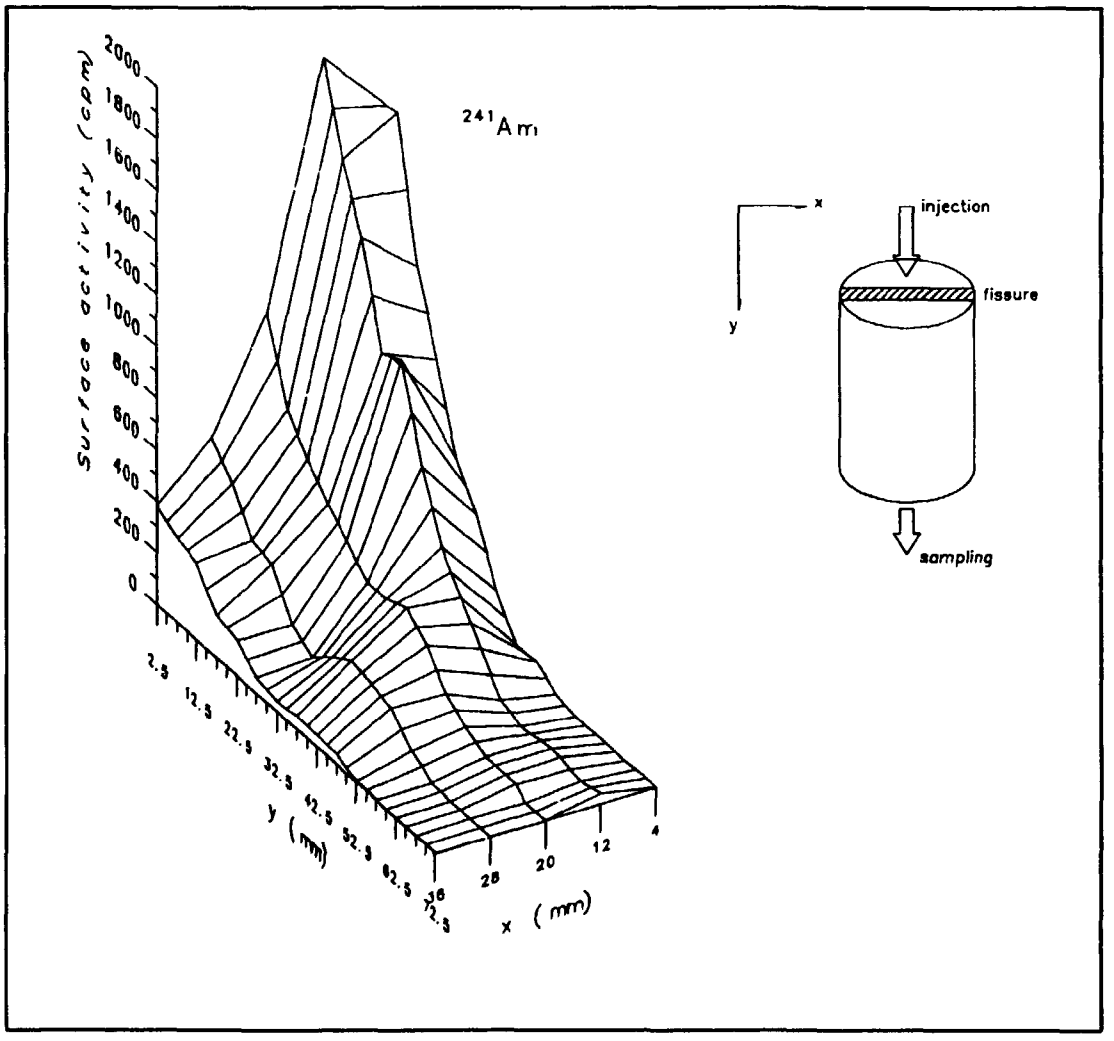

Figure 2.5 Spatial distribution of ^{241}Am on the fissure surface after 122.4 hours of tracer flow through the fissure.

2.5 Supporting Data

Results from the complementary sorption experiments, using crushed granite and fissure-filling materials from the same location as the cores used in the tracer experiments, were available as cation exchange capacity and distribution ratios (amount sorbed/amount in solution) [8]. The cation exchange capacity of crushed granite and the distribution ratio of ^{85}Sr as a function of 1/d (d is the mean diameter of the particle size range) are shown in Figures 2.6 and 2.7, respectively. From these types of graphs, distribution ratios for sorption of ^{85}Sr, ^{134}Cs and ^{152}Eu to the inner surfaces and to the outer surfaces of the rock materials were evaluated. Distribution ratios versus contact time were also available.

Additional information about the Stripa granite, such as geological, geochemical, and geophysical data, can be found in the general information reports from the Stripa Project [11,12,13,14].

2.6 Error Estimates

The errors associated with the analysis of the lignosulphonate concentrations were estimated to be about ±2% in the optical absorption data. The error in each activity measurement is given by $N^{0.5}$, where N is the number of counts. The flow rates were measured several times during each run, and the variation in flow rate during a run was less than ±2%.

In the experiments the rock cores were clamped by two steel bands , and the outer surfaces were covered with a coating of urethane lacquer. Hence the rock samples were not 100% rigidly fixed, which may have caused some slight variation in the flow paths in the fractures. Another possible source of error is that air bubbles may have formed in the system.

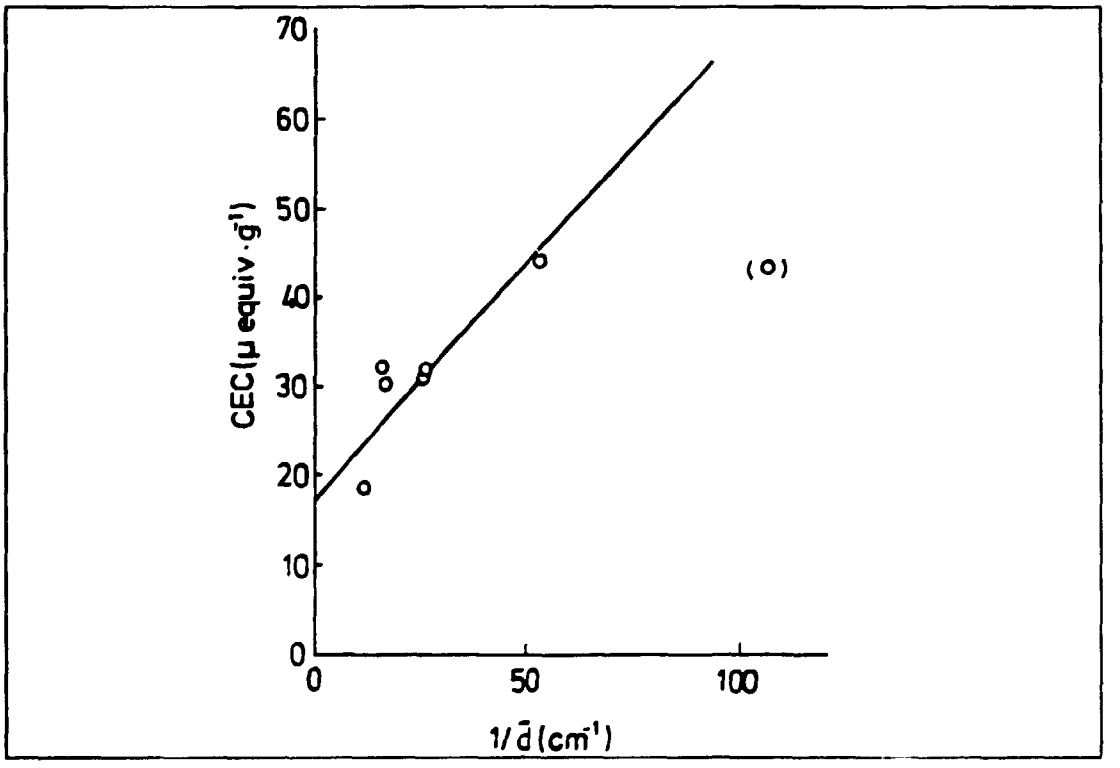

Figure 2.6 Cation exchange capacity (CEC) as a function of 1/d, where d is the mean diameter of the particle size fraction.

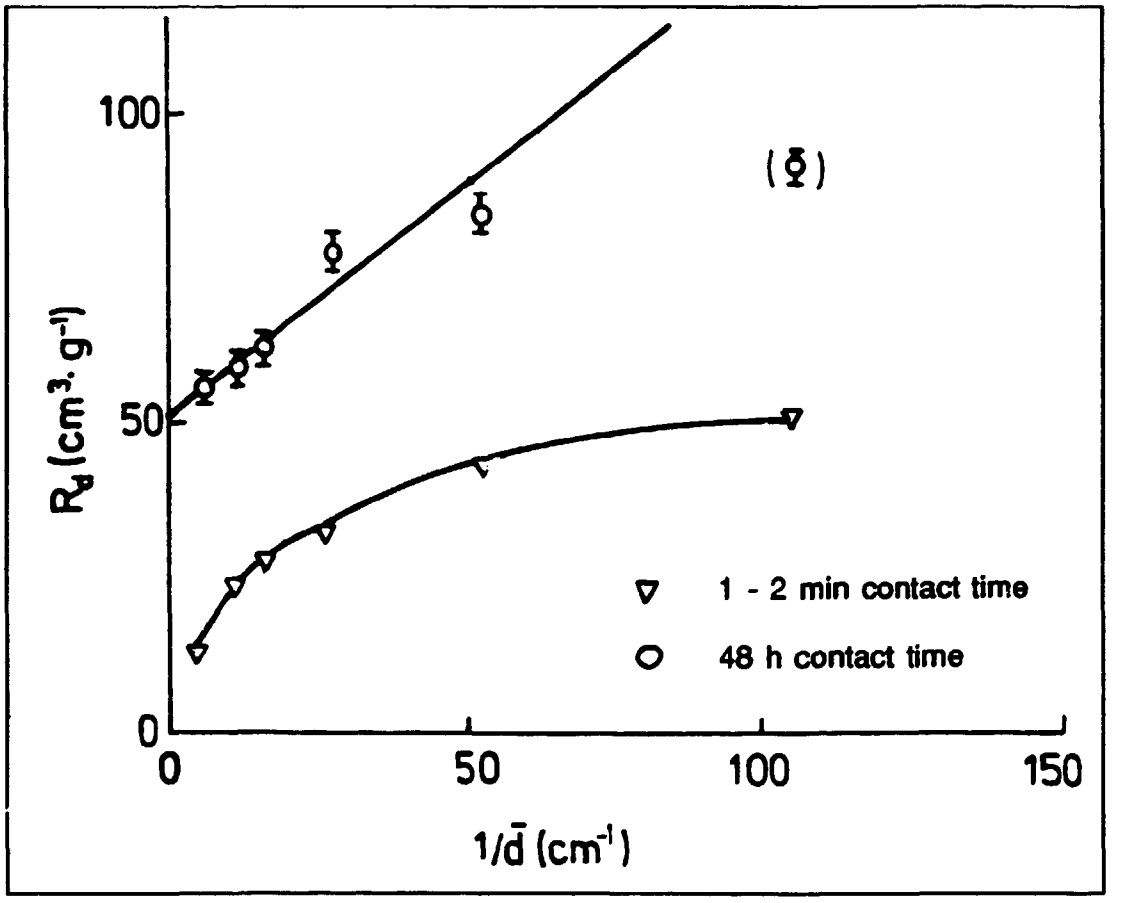

Figure 2.7 Distribution ratio (R_d) for ^{85}Sr as a function of 1/d, where d is the mean diameter of the particle size fraction.

3. Validation Methodologies

All the project teams working with this test case used a similar approach involving:
- review of data,
- calibration of models against data
- calibration assessment,
- check of parameters for physical reasonableness, and
- comparison of alternative models.

The results from the experiments with the moderately sorbing tracers were used to calibrate their models. The KTH Project Team [10] used models describing migration in a fracture including advection, dispersion and molecular diffusion into the rock matrix. These models were calibrated against experimental data from runs with non-sorbing tracers. The best estimates of the hydraulic parameters were used in a model that also included sorption. This model was calibrated against results from experiments with sorbing tracers. The estimated sorption parameters were compared with results from independent sorption measurements. A comparison was made between two ways of modelling velocity variations in the fracture: hydrodynamic dispersion and channelling dispersion. An experimental design was also identified which would facilitate the distinction between the two models.

The JAERI Project Team [15] applied a conceptual model including advection, dispersion, sorption and diffusion from the fracture into the rock matrix. Similarly to the KTH team, two different dispersion mechanisms were tested: hydrodynamic dispersion assuming a constant fracture aperture, and channelling dispersion with a varying fracture aperture. Both models were calibrated against runs with non-sorbing and moderately sorbing tracers, and the estimated parameter values were compared.

The PNL Project Team [16] used the same conceptual model as the other teams including advection, dispersion, sorption and diffusion from the fracture into the rock matrix. The model was calibrated against results from an experiment where the moderately sorbing tracer strontium was used. The sensitivities of the model parameters to variables in the experimental design were also determined with the aim of assessing whether improvements in the experimental design could be made in order to minimise the uncertainty in the parameter values. A model without matrix diffusion was also calibrated against the same experimental data, and were compared with the results for the model with matrix diffusion.

4. Models

4.1 Mathematical Models and Assumptions

One model that was used by all Project Teams working with this test case describes advective solute transport in a fracture with constant aperture. The model considers longitudinal hydrodynamic dispersion in the fracture, sorption onto the fracture surface, diffusion from the fracture into the porous rock matrix, and sorption within the rock matrix. Sorption both on the fracture surface and within the rock matrix was assumed to be linear, and instantaneous.

The equation that describes the transport in the fracture is:

$$R_f \frac{\partial c_f}{\partial t} = D_L \frac{\partial^2 c_f}{\partial x^2} - v_f \frac{\partial c_f}{\partial x} - R_f \lambda \cdot c_f + \frac{2D_e}{\delta} \frac{\partial c_p}{\partial z}\bigg|_{z=0} \tag{1}$$

where c_f = tracer concentration in the fluid in the fracture [M/L^3]
c_p = tracer concentration in pore water in the matrix
D_L = dispersion coefficient [L^2/T]
v_f = fluid velocity in the fracture [L/T]
D_e = effective diffusivity in the pores in the matrix [L^2/T]
δ = fracture aperture [L]
t = time [T]
λ = decay constant [T^{-1}]
x = distance along fracture [L]
z = distance into rock matrix [L]

R_f is the retardation in the fracture due to sorption on the fracture surface:

$$R_f = 1 + \frac{2K_a}{\delta} \tag{2}$$

where K_a [L] is the surface distribution coefficient.

The equation describing the transport in the matrix perpendicular to the fracture is:

$$\frac{\partial c_p}{\partial t} = \frac{D_e}{\varepsilon_p \cdot R_m} \frac{\partial^2 c_p}{\partial z^2} - \lambda \cdot c_p \tag{3}$$

where the retardation in the matrix due to sorption in the matrix is:

$$R_m = 1 + \frac{K_d \cdot \rho_b}{\varepsilon_p} \tag{4}$$

and K_d = bulk distribution coefficient [L^3/M]
ε_p = matrix porosity [L^3/L^3]
ρ_b = matrix bulk density [M/L^3]

The relation between the effective diffusivity, D_e, and the pore water diffusion coefficient, D_p, is:

$$D_e = D_p \cdot \varepsilon_p \tag{5}$$

and, according to the KTH project team, the relation between the pore water diffusion coefficient, D_p, and the molecular diffusivity, D_M, is:

$$D_p = D_M \frac{\delta_D}{\tau_{KTH}^2} \tag{6}$$

where δ_D = constrictivity of the pores, and
τ_{KTH}^2 = "tortuosity" of the pores,

while the PNL project team defines the relation as:

$$D_p = D_M \cdot \tau_{PNL} \tag{7}$$

where τ_{PNL} = "tortuosity" of the pores, which is of course different from the tortuosity as defined by KTH.

Those are just two different ways to define a geometrical factor which accounts for the non-uniformity and winding of the pores in the matrix.

The teams from KTH and PNL studied the effect of omitting matrix diffusion and matrix sorption from the model.

The KTH and JAERI Project Teams [10,15] also used models with a variable fracture aperture. Thus the flow occurs in channels and dispersion of the solute is caused by the velocity differences in the channels. Sorption to the fracture surface, diffusion into the rock matrix, and sorption within the rock matrix were also considered in these variable fracture-aperture models. Both Project Teams further assumed that hydrodynamic dispersion in each channel is negligible compared to the dispersion caused by the different residence times in different channels. The transport in each channel is given by Eq.1, neglecting the hydrodynamic dispersion term.

The KTH Project Team [10] assumed that the fracture apertures have a lognormal distribution and that the channels are parallel with negligible interconnection between the different channels. The density function is given by:

$$f(\delta) = \frac{1}{\sigma(2\pi)^{1/2}} \frac{1}{\delta} \exp\left[- \frac{[\ln(\delta/\mu)^2]}{2\sigma^2} \right] \tag{8}$$

where μ = mean of fissure aperture in the lognormal distribution [L], and
σ = standard deviation in the lognormal distribution.

The solute transport is assumed to occur with different velocities in the channels, and the experimentally determined breakthrough curve is assumed to be the combination of the mixed effluent from all channels according to:

$$\frac{c(t)}{c_0} = \frac{\int_0^\infty f(\delta)\, Q(\delta)\, c_f(\delta,t)\, d\delta}{\int_0^\infty f(\delta)\, Q(\delta)\, d\delta} \tag{9}$$

where $c_f(\delta,t)$ is the breakthrough curve for each channel and $Q(\delta)$ is the flow rate in each channel.

The JAERI Project Team [15] used a two-dimensional model to describe the flow field in the fracture. The fracture plane was divided by a rectangular grid into nodes with different apertures. A lognormal distribution of the fracture apertures was assumed. Furthermore it was assumed that the water could be stagnant in parts of the fracture. This was modelled by assuming a fracture porosity less than 1. The equations used to describe the flow between two adjacent nodes i and j, Q_{ij}, with apertures δ_i and δ_j are:

$$Q_{ij} = k_{ij} (P_i - P_j) \tag{10}$$

$$k_{ij} = \frac{\phi g}{6\nu} \frac{\Delta y}{\Delta x} \left(\frac{1}{\delta_i^3} + \frac{1}{\delta_j^3} \right)^{-1} \tag{11}$$

where P = head in the node [L]
k = transmissivity between the nodes [L^2/T]
ν = viscosity of fluid [L^2/T]
Δx = grid size in the direction of overall flow [L]
Δy = grid size in the direction perpendicular to overall flow [L]
ϕ = fracture porosity, i.e. part of the channel where water is flowing [L^3/L^3]
g = gravitational acceleration [L/T^2]

Solute transport through the fracture was calculated using a particle-tracking method. Particles were introduced in the known steady-state flow field at the fracture inlet and moved with the flow. Particles coming to an intersection were distributed among the outlet channels with a probability proportional to the flow rates.

The upstream boundary condition used by the Project Teams is a constant tracer concentration at the inlet during tracer injection. All the Project Teams obtained an effective downstream boundary condition in the following manner. The equations were solved in a much larger domain with the downstream boundary condition taken as zero concentration. Then the model output was taken to be the concentration at a distance from the upstream boundary corresponding to the length of the core used in the experiment.

4.2 Codes

The KTH Project Team [10] used an analytical solution to the advection-dispersion equation with sorption and matrix diffusion for the case with a constant fracture aperture. For the case with varying fracture aperture, an analytical solution to the transport equation without hydrodynamic dispersion was used to calculate the breakthrough curve for each channel. The determination of parameters was done by means of a non-linear least-squares fitting.

The JAERI Project Team [15] used semi-analytical solutions to the model with a constant fracture aperture. In the particle tracking method, used when assuming a variable fracture aperture, the fracture plane was modelled as a rectangular network system. A one-dimensional solution to the transport equation was used to calculate the travel time of each particle in a channel. Best-fit parameter values were obtained by visually comparing calculated and experimental breakthrough curves.

The PNL Project Team [16] used a code named CRACKMAT, which is an implementation of the analytical solution to the advection-dispersion equation for solute transport in a fracture, accounting for sorption, matrix diffusion and radioactive decay. CRACKMAT was coupled to CRK1 and NLFIT, which are programs that implement the parameter estimation method used. The routine CRK1 checks for parameter bounds and calculates the model's sensitivity coefficients at a given set of time with the current set of parameter values. NLFIT uses a non-linear weighted least-squares method, the Levenberg-Marquardt algorithm, for parameter estimation.

5. Results

5.1 Data review

A large amount of data from runs with both non-sorbing and sorbing tracers was available to the modellers as well as results from independent sorption measurements. However, the transport of non-sorbing and sorbing tracers were studied in separate experiments, which may have made it more difficult to determine flow paths if the fracture properties changed between the experiments. A simultaneous injection of a non-sorbing and sorbing tracer would have improved the possibilities to determine the flow parameters independently of the sorption [16].

The JAERI Project Team [15] observed that flow velocities estimated by Neretnieks et al. [9], information which was available to the Project Teams, were not proportional to pumping rates in the experiments. They interpreted that as being a result of the presence of areas with stagnant water in the fracture which expand in inverse proportion to the water flux.

The JAERI Project Team [15] also noted that there are plateaux in the experimental breakthrough curves which indicate channel transport in the fracture.

During the course of the INTRAVAL study some questions were raised regarding the data provided. One question concerned some of the strontium runs where the effluent concentration at the onset of the experiment indicated the presence of residual activity from an earlier experiment in the actual core. Also error estimates and sources of errors were requested and have been provided by the pilot group (see section 2.6). Some misunderstandings regarding the injection flow rates and flushing flow rates given to the modellers were also resolved in communications with the pilot group. This shows the importance of interaction between the experimentalists performing the experiments and the modellers evaluating the results.

5.2 Calibration and Prediction

The KTH Project Team [10] determined hydraulic parameters by calibrating both the hydrodynamic dispersion model and the channelling dispersion model using experimental breakthrough curves for non-sorbing tracers. The parameters obtained were used in fitting the models to experimental breakthrough curves for sorbing tracers. This means that no actual prediction was made since the parameters describing the interaction with the rock were determined by a fitting procedure instead of using independently determined values of these parameters and predicting the experimental breakthrough curves. However, the fitted values of the rock interaction parameters were compared with independently measured values reported in the literature.

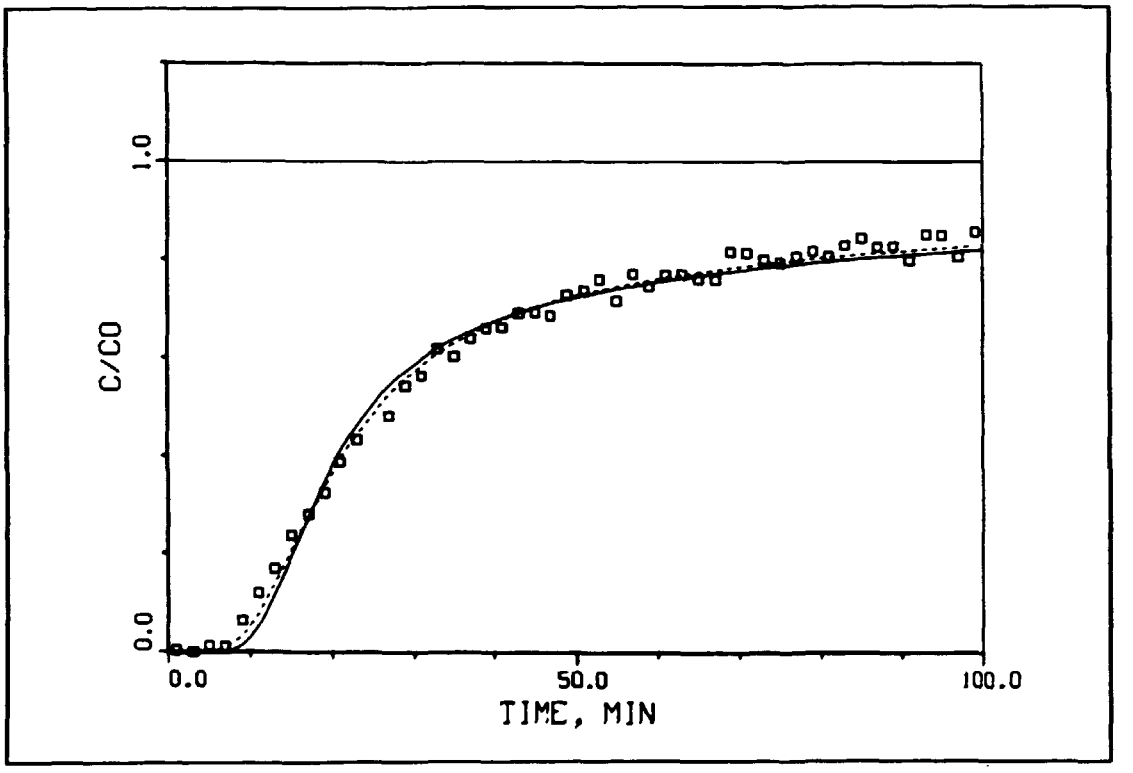

Figure 5.1 Curves fitted with the hydrodynamic dispersion model (solid line) and channelling model (dashed line) for strontium in core 5, KTH team [10].

Curves fitted with the two models and the experimental breakthrough curve from a run with the sorbing tracer strontium in core 5 are shown in Figure 5.1. The two models give very similar results (see also section 5.3). The effect of omitting different mechanisms in the hydrodynamic dispersion model was also studied by fitting the model neglecting the interaction with the rock matrix to experimental data for sorbing tracer (Figure 5.2). From the results it was concluded that it is not possible to explain the behaviour of strontium in the fracture without considering matrix diffusion and sorption within the rock matrix. Predictions of breakthrough curves for other experimental conditions were also made in order to determine an experimental design that would facilitate the distinctions between the hydrodynamic dispersion model and the channelling model.

The JAERI Team [15] used values of the flow velocity, fracture aperture and dispersion length from an evaluation of the experiments made by Neretnieks et al. [9] as part of the experimental programme, and calibrated breakthrough curves calculated with the constant aperture model with experimental data from runs with sorbing tracers. This was done to obtain best-fit values of the parameters describing the tracer-rock interaction. The variable aperture model was calibrated against experimental breakthrough curves for the non-sorbing tracer HTO. Based on the shape of the experimental breakthrough curves, a fracture aperture distribution that reproduced solute transport in two channels was selected. The distribution of flow rates in this realisation is shown

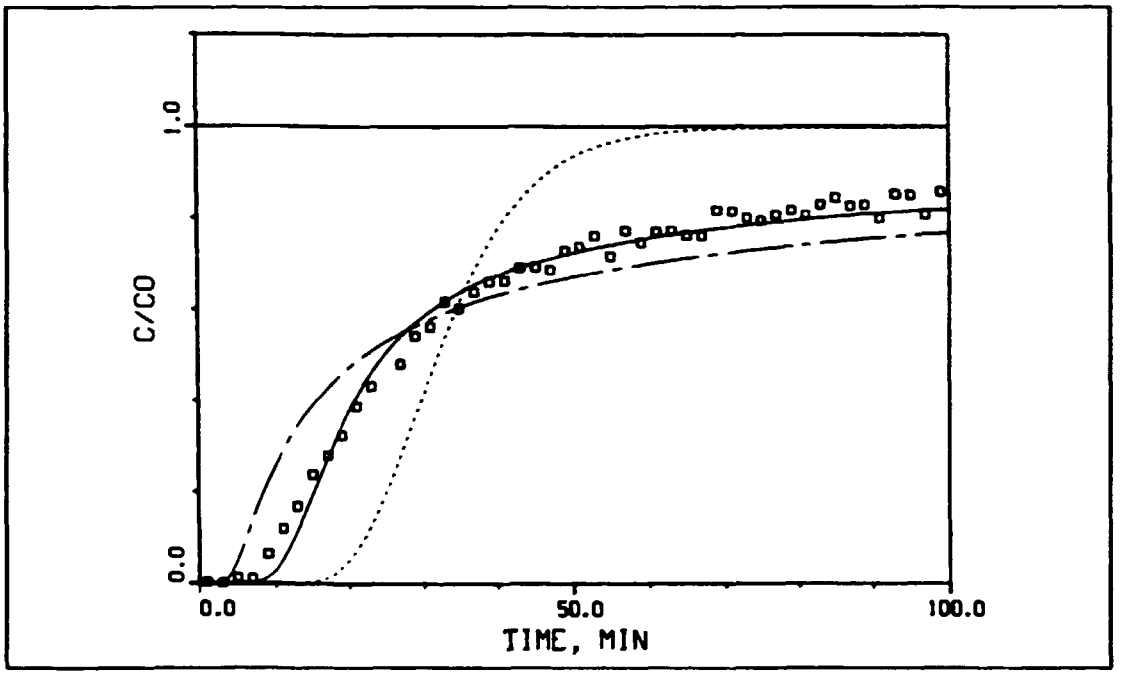

Figure 5.2 Curve fitted using the hydrodynamic dispersion model for strontium (solid curve). Dashed curve; omitting matrix diffusion and matrix sorption. Long-dashed curve; omitting fracture surface sorption. KTH team [10].

in Figure 5.3. The best-fit to the experimental data resulted in a fracture porosity that was proportional to the ratio of the water flux and the tracer velocity in the fracture. It was concluded that the variable fracture aperture resulted in curves that fit the experimental data somewhat better than the curves produced by the constant aperture model. Examples of best-fit curves are shown in Figure 5.4. Best-fit values of the parameters describing the interaction with the rock was produced by calibrating against data from experiments with sorbing tracers. No predictions were made with either of the models.

The PNL Project Team [16] calibrated the advection-dispersion model with matrix diffusion against an experimental breakthrough curve for the sorbing species strontium to obtain best-fit values of the dispersion coefficient, the water velocity in the fracture, the fracture aperture and the retardation of the tracer in the fracture. The effect of time-averaging of the effluent concentration was investigated by fitting the experimental data to models simulating sampling of the effluent every 60, 120 and 240 s as well as instantaneously. The time-averaged concentrations obtained from sampling every 60 and 120 s were found not to be appreciably different from those obtained from instantaneous sampling (Figure 5.5). Since the sampling interval in the experiment was 120 s, it was concluded that the breakthrough curve can be fitted to an instantaneous sampling model in this case.

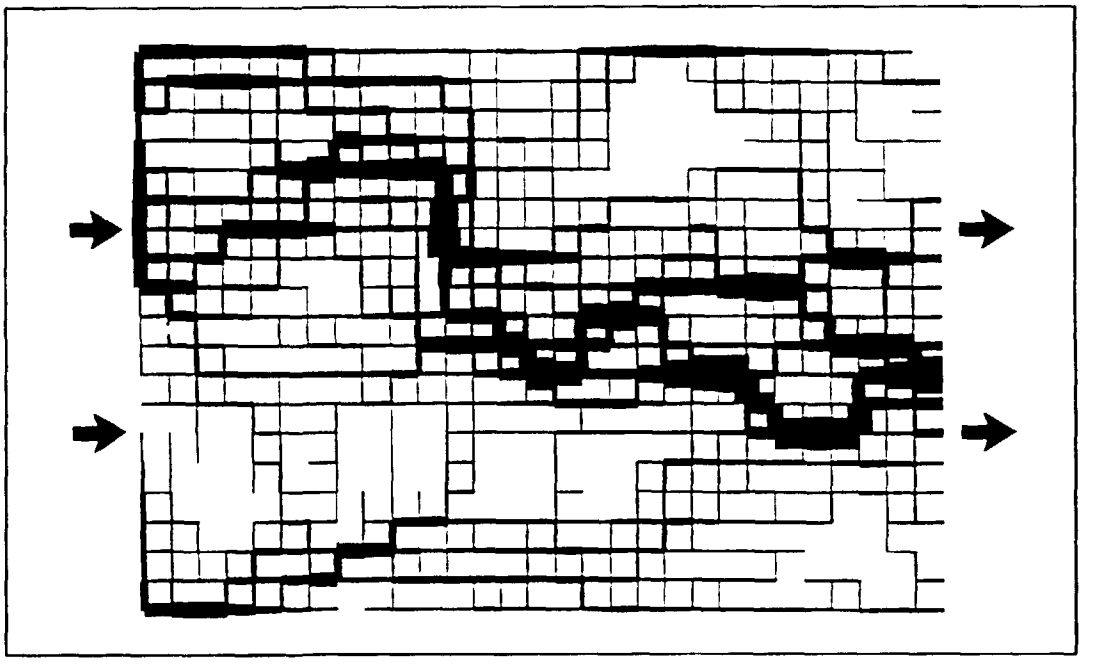

Figure 5.3 Distribution of flow rates in the variable aperture model according to the JAERI Team [15].

5.3 Parameter Assessment

A very large number of breakthrough curves were available. Not all of these curves were used. Further, different teams generally used different curves. This makes it rather difficult to compare the results from all teams. However, the KTH team [10] used the runs in cores 5 and 6, and the PNL Project Team [16] used one of the strontium runs in core 5 in their analysis. The JAERI Project Team [15] used the data from experiments in core L.

There are too many unknown parameters in the transport equation to obtain a unique interpretation of each parameter by curve fitting. At best, only combinations of the parameters can be determined by fitting the breakthrough curves. Therefore the Project Teams produced best-fit values for these combinations of parameters, or assigned values based on data found in the literature to some of the parameters.

The KTH Project Team [10] determined best estimates of the Peclet number and the water residence time for the hydrodynamic dispersion model by fitting the breakthrough curves for non-sorbing tracer. The effective diffusivity in the matrix was assigned a value based on experimentally determined diffusivities reported in the literature. From the water residence time and the measured flow rate, the average fracture aperture was calculated, and the dispersion coefficient was calculated from the Peclet number. The best-fit values of the Peclet number and the fracture aperture were used in the modelling of the runs with sorbing tracer. In these runs the tracer residence-time and a parameter which takes into account the interaction with the rock

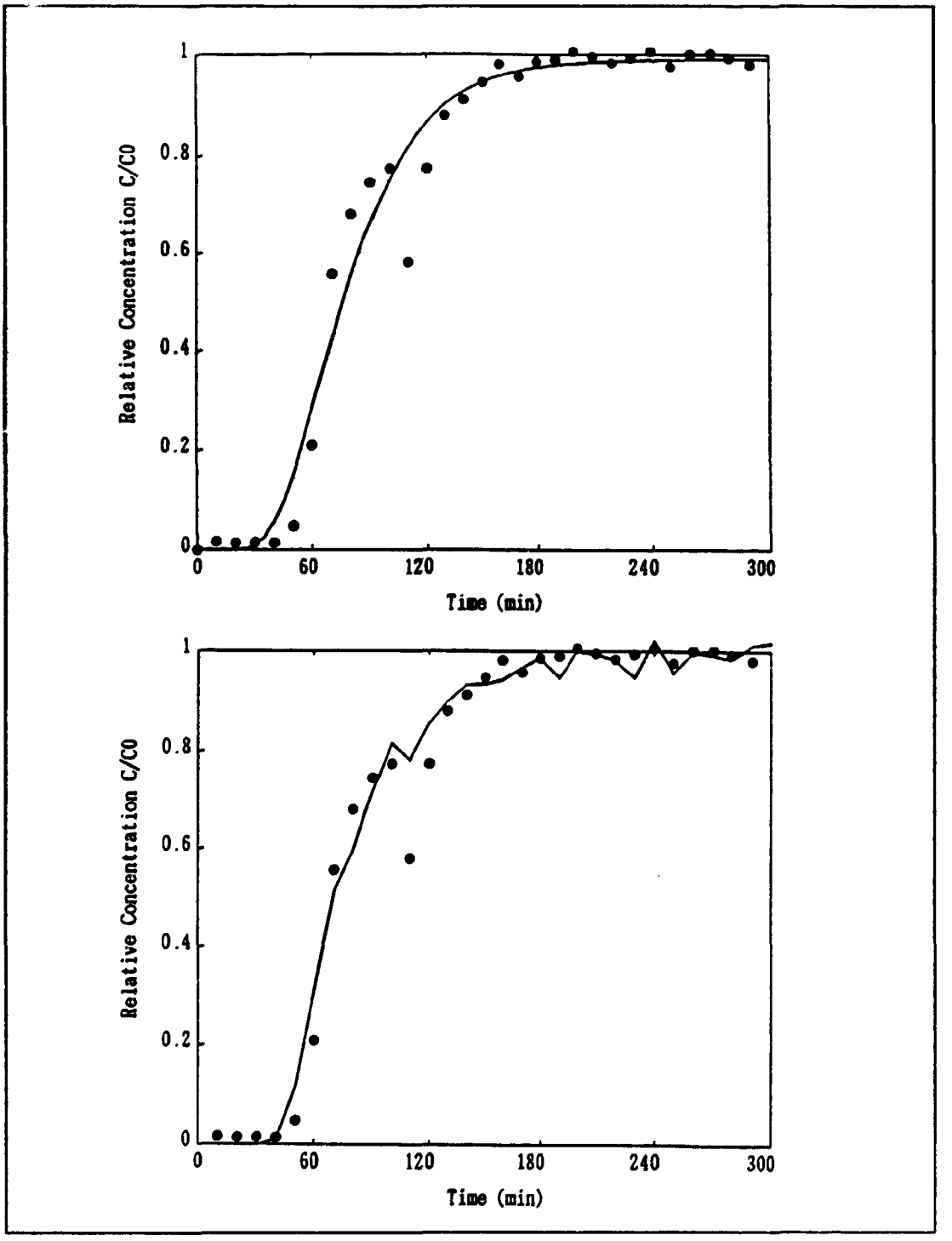

Figure 5.4 Experimental and calculated breakthrough curve for HTO in core L, JAERI Team [15]. Upper; constant aperture model. Lower; variable aperture model.

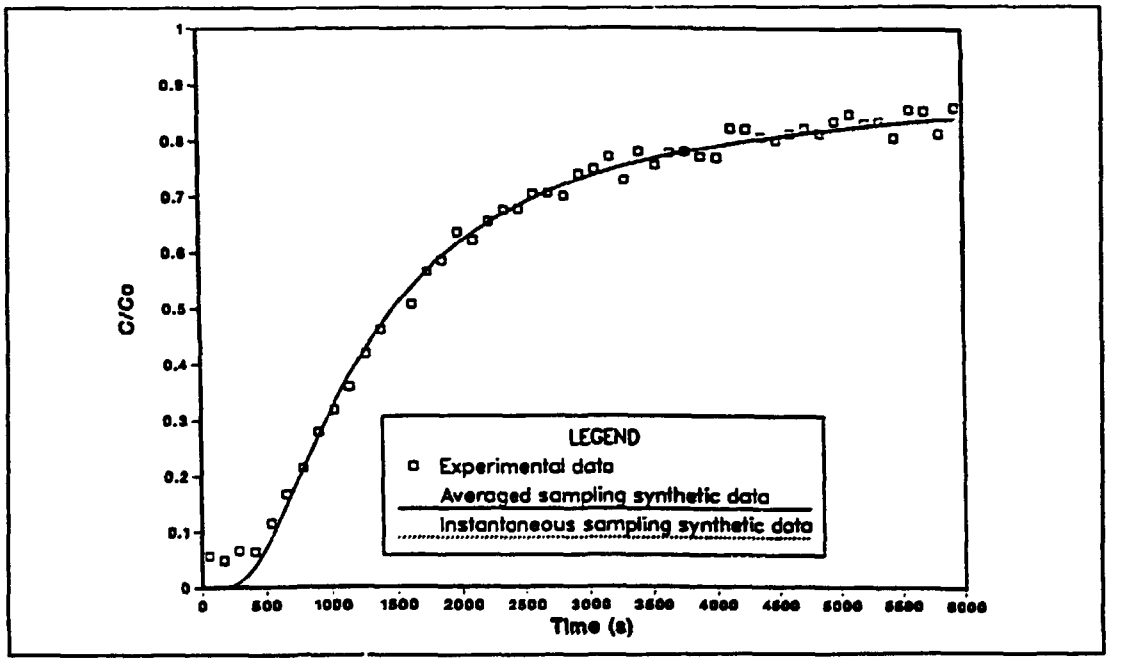

Figure 5.5 Best-fit comparison of instantaneous and time-averaged sampling. The 2 curves almost completely overlap each other in the figure.

matrix were determined by data fitting. For the channelling dispersion model, the Project Team determined best-fit values of the standard deviation in the lognormal distribution of the fracture aperture and the water residence-time using breakthrough curves for the non-sorbing tracers. The tracer residence-time and the parameter accounting for the interaction with the rock matrix were determined using the results from the sorbing tracer experiments. Obtained best-fit parameter values from experiments with the non-sorbing lignosulphonate ion and sorbing tracer strontium in core 5 are given in Table 5.1.

The PNL Project Team [16] calculated initial values for the model parameters and coefficients from values reported in [10], and assigned values for matrix tortuosity, Peclet number and free solution diffusivity of the tracer. The best-fit parameter estimates obtained by using the results from one of the experimental runs with strontium in core 5 are given in Table 5.1 together with the best-fit parameter estimates obtained by the KTH Project Team. From the table it can be seen that the best estimates of the fracture aperture produced by the two teams are very close. To be able to compare the best-fit values of the fracture sorption parameters, Eq.2 has been used to calculate the fracture retardation from the KTH best-fit data, and the fracture surface sorption coefficient from the PNL best-fit data. This shows that the two teams have arrived at values of the sorption parameters that are in fair agreement. The best-fit parameter estimates for instantaneous and time-averaging sampling models are given in Table 5.2 for the curves in Figure 5.5. The table shows that the values for the parameters were not significantly different between the fits, and that the values of the fracture aperture and fracture retardation are similar to those obtained by the KTH project team (Table 5.1)

Table 5.1 Best-Fit Parameter Values from Experiments in Core 5 [10,16].

Parameter	KTH Project Team Hydrodynamic Dispersion	KTH Project Team Channelling Dispersion	PNL Project Team Hydrodynamic Dispersion
Core 5, mean values			
Fracture aperture, δ, [mm]	0.14	0.14	
Peclet number, $v_f x/D_L$	20		
Standard deviation in aperture distribution, σ		0.155	
Fracture surface sorption coefficient, K_a, [m]	$28.3 \cdot 10^{-5}$	$34.7 \cdot 10^{-5}$	
Rock matrix interaction parameter, $D_e K_d \rho_b$, [m^2/s]	$6.4 \cdot 10^{-11}$	$5.3 \cdot 10^{-11}$	
Fracture retardation, R_f	4.0*	5.0*	
Core 5, strontium, run 514			
Fracture aperture, δ, [mm]			0.13
Dispersion coefficient, D_L, [m^2/s]			$2.9 \cdot 10^{-5}$
Fracture velocity, v_f, [m/s]			$1.0 \cdot 10^{-3}$
Fracture surface sorption coefficient, K_a, [m]	$27 \cdot 10^{-5}$	$34 \cdot 10^{-5}$	$37 \cdot 10^{-5}$**
Rock matrix interaction parameter, $D_e K_d \rho_b$, [m^2/s]	$10.1 \cdot 10^{-11}$	$8.8 \cdot 10^{-11}$	
Fracture retardation, R_f	3.9*	4.9*	6.7

* calculated using Eq.2 and best-fit values of fracture surface sorption coefficient and fracture aperture
** calculated using Eq.2 and best-fit values of fracture retardation and fracture aperture

Table 5.2 Homogeneous measurement error (HME) and best-fit parameter estimates for instantaneous and time-averaged sampling models [16].

Parameter	Instantaneous	Time-averaged
HME	$2.12 \cdot 10^{-2}$	$2.07 \cdot 10^{-2}$
Fracture aperture, δ, [m]	$0.125 \cdot 10^{-3}$	$0.136 \cdot 10^{-3}$
Dispersion coefficient, D_L, [m^2/s]	$2.999 \cdot 10^{-5}$	$3.133 \cdot 10^{-5}$
Fracture velocity, v_f, [m/s]	$1.029 \cdot 10^{-3}$	$0.980 \cdot 10^{-3}$
Fracture retardation, R_f	6.05	6.00
Matrix porosity, ε_p	$6.106 \cdot 10^{-2}$	$6.276 \cdot 10^{-2}$
Matrix retardation, R_m	13024	12692

The JAERI Project Team [15] used the experimental breakthrough curves determined for core L. The team selected the same values of the flow velocities as previously evaluated from these experiments by Neretnieks et al. [9] in combination with a fracture aperture of $0.18 \cdot 10^{-3}$ m and a dispersion length of 0.025 m, and simulated the breakthrough curves for the non-sorbing tracer tritiated water using the constant aperture model. In applying the variable fracture aperture model, values were assigned to the standard deviation in the aperture density distribution (0.25), to the correlation length (0.05 m) and to the mean fracture aperture ($0.1 \cdot 10^{-3}$ m). These values were selected in order to reproduce transport through two main channels. For runs with a low flow rate, best-fits were obtained with a fracture porosity less than one. The Project Team concluded that this could be due to larger areas in the fracture with stagnant water at lower flow rates.

By using the experimental breakthrough curves for the sorbing species strontium and cesium, best-fit values of the fracture retardation factor and the matrix retardation factor were estimated. The best-fit values of fracture- and matrix-retardation for strontium obtained using the constant-aperture model were larger than those obtained using the variable aperture model. The range of the values obtained from the 7 runs are:

	Constant aperture model	Variable aperture model
Fracture retardation, R_f	3.0 - 5.0	2.0 - 3.0
Matrix retardation, R_m	14000 - 18000	4500 - 12000

The JAERI team has calibrated their models against strontium runs in core L while the KTH team and PNL team used data from strontium experiments in core 5. The cores differ in size, both in diameter and length. The diameter of core L was 20 cm and the length was 30 cm, while the diameter and length of core 5 was 10 and 18 cm, respectively. This difference in size seems not

to effect sorption to any greater extent since the obtained best-fit values of both fracture retardation and matrix retardation in the cores are in good agreement (see Tables 5.1 and 5.2).

For the 6 cesium runs the following ranges of best-fit values were obtained:

	Constant aperture model	Variable aperture model
Fracture retardation, R_f	4.0 - 5.0	3.0 - 4.0
Matrix retardation, R_m	30000 - 150000	25000 - 90000

For two of the cesium runs the implied matrix retardation was markedly lower than for the remaining runs. The team concluded that this could be due to non-linear sorption of cesium since the injection concentration of cesium in these two runs was about two times higher than in the other runs.

The best-fit values of the fracture surface sorption coefficient and fracture retardation obtained by the different teams can be compared with results from independent sorption measurements on crushed granite from the same location as the cores, i.e. the Stripa mine. Values of the surface sorption coefficient for strontium of $(3.08 \pm 1.25)10^{-5}$ m has been reported by Eriksen et al. [8], and a value of $6.6 \cdot 10^{-5}$ m by Skagius et al. [17]. These values are about 5 to 10 times lower than the best estimates by the KTH and PNL project teams (Table 5.1).

The fracture retardation of strontium corresponding to the independent measured surface sorption coefficients in case of a fracture aperture of $0.18 \cdot 10^{-3}$ m as assumed by the JAERI team is, according to Eq.2, 1.34 ± 0.14 and 1.7, respectively. These values are less than 5 times lower than the best estimates by the JAERI team. Reported values of independent measured surface sorption coefficients for cesium on crushed Stripa granite are $(25.9 \pm 2.7)10^{-5}$ m [8] and $12 \cdot 10^{-5}$ m [17]. With the fracture aperture assumed by the JAERI team these values correspond to fracture retardation of 3.88 ± 0.30 and 2.3, respectively, i.e somewhat lower than the best estimate values by the JAERI team.

5.4 Sensitivity and Uncertainty Analysis

The PNL Project Team [16] performed a sensitivity analysis for all the model parameters by calculating the sensitivity coefficients about the best-fit values of the parameters. This was done for the original experimental set up, and also for a sample three times as long as the sample in the experiment in order to assess whether a using a longer core in the experiment would reduce the uncertainty associated with the estimated parameter values. It was shown that for a longer core the model sensitivity to velocity, fracture aperture, matrix porosity and matrix retardation increased. This would imply that the uncertainty in the best-fit values of these parameters was decreased.

5.5 Statistical Analysis

The PNL Project Team [16] used residual plots as a qualitative way to discriminate between competing or plausible models. Synthetic data were generated using the best-fit parameter values in the advection-dispersion model with matrix diffusion, then the model without matrix diffusion was fitted to the synthetic data (Figure 5.6). The difference in concentration between the synthetic curve and the fitted curve was calculated. These residuals exhibit a marked trend implying a systematic error caused by using an incorrect model. The model without matrix diffusion was also fitted to the original experimental data (Figure 5.7). A similar trend in the residuals was found, which was interpreted as a systematic error due to the use of a model without matrix diffusion.

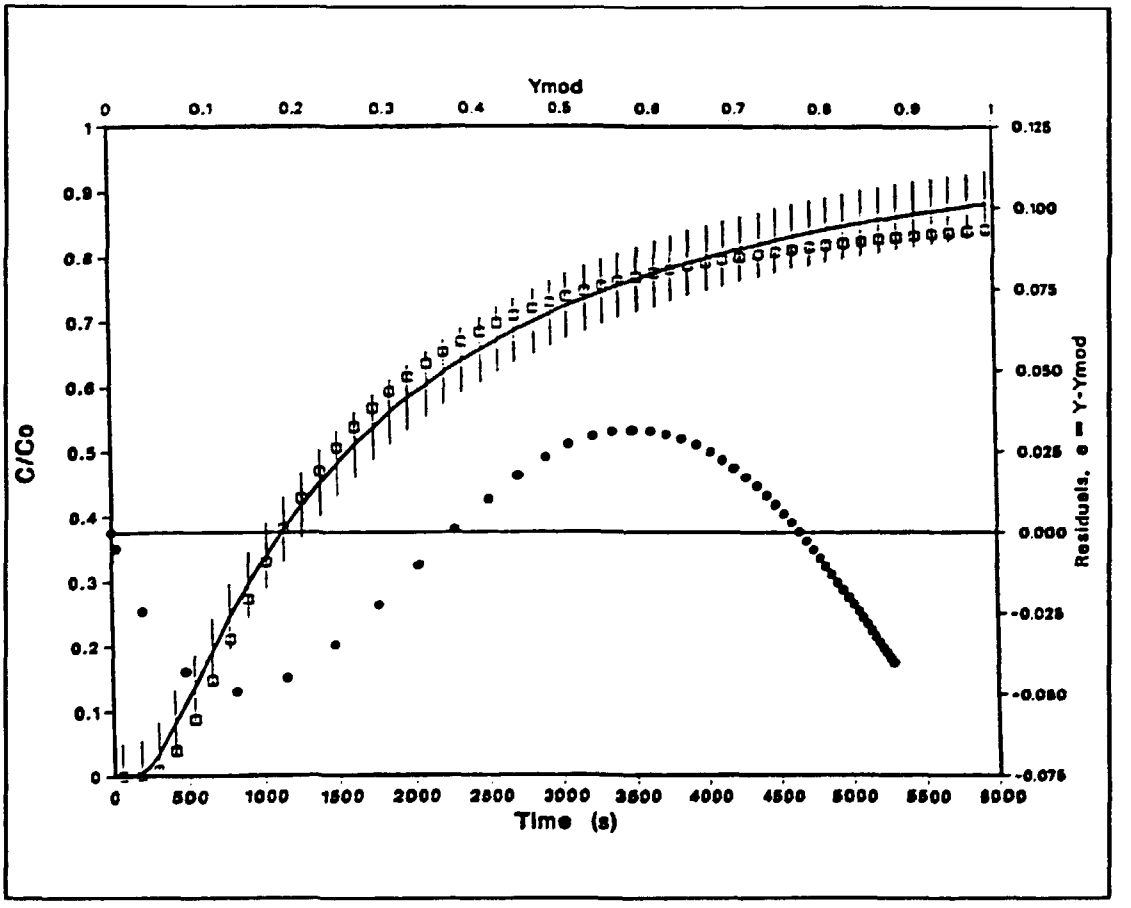

Figure 5.6 Model without matrix diffusion fitted to synthetic data generated with model including matrix diffusion, PNL Team [16]. The residuals, right y-axis, are plotted against the predicted value of C/C_0 on the top axis.

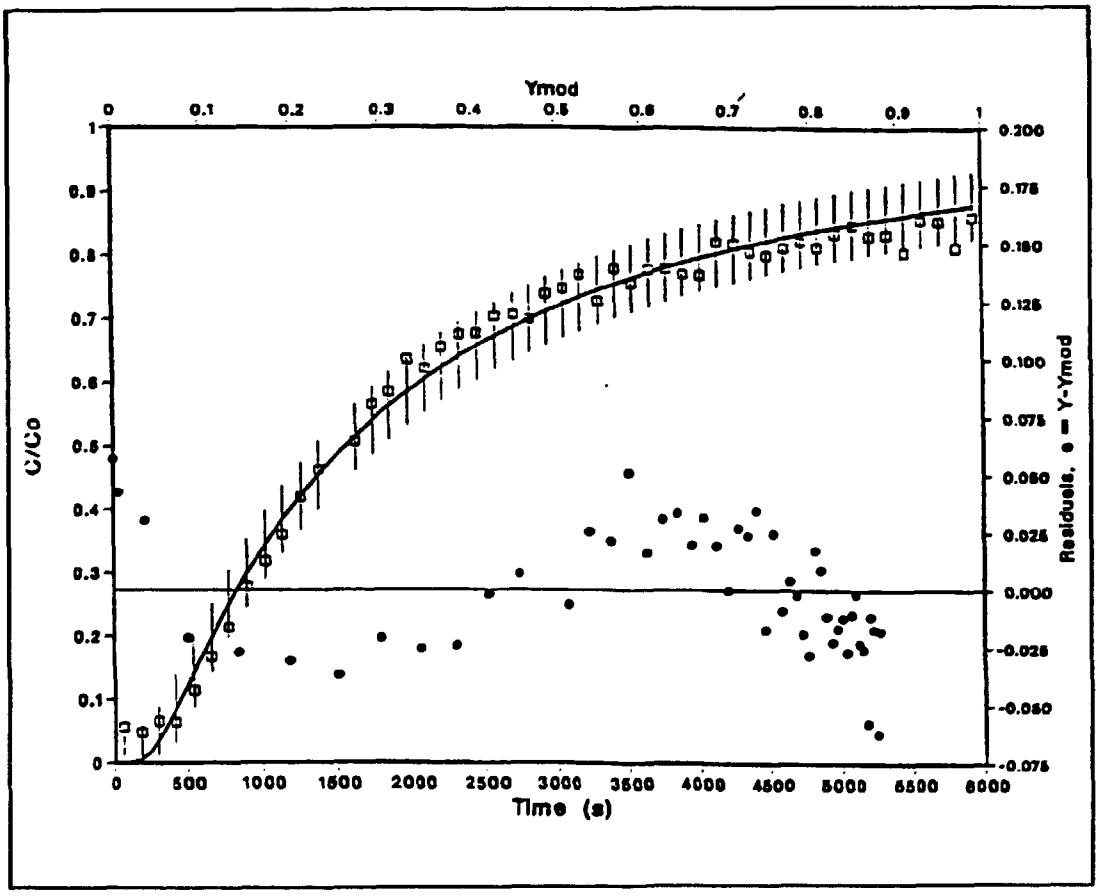

Figure 5.7 Model fit without matrix diffusion to experimental data, PNL Team [16]. The residuals, right y-axis, are plotted against the predicted value of C/C_0 on the top x-axis.

6. Conclusions

6.1 Conclusions on Validation Methodology

In the context of repository performance assessment the approach to validation generally involves several activities, which are all important. These are:
- review of models and data,
- calibration of a model against part of the data and assessing the calibration,
- making predictions and comparing these with the rest of the data,
- analysis of discrepancies,
- comparison of alternative models,
- assessing implications for performance assessment, and
- suggestions for further experiments.

The methodology adopted by the Project Teams working with this test case involves several of these activities. However, none of the teams have performed any prediction and testing of the predictions against experimental data. Without this it is difficult to draw any strong conclusions regarding the validity of the models.

6.2 Conclusions on Models

The processes included in the models that have been applied to this test case are advection, dispersion, sorption to the fracture surface, matrix diffusion and sorption within the rock matrix. The models without matrix diffusion and sorption within the rock matrix gave poor fits to the experimental data [10] or residuals with a trend [16] which implies a poor model. The KTH Project Team [10] also concluded that in a model with matrix diffusion the best-fit values of the parameters determining the interaction between tracer and rock were in fair agreement with independently measured sorption and diffusivity data. These results suggest the need to include matrix diffusion and matrix sorption in models to represent data for this test case.

The KTH Project Team [10] concluded that it was not possible to distinguish between the two dispersion mechanisms studied: hydrodynamic dispersion and channelling dispersion. Equally good fits were obtained with both models. The JAERI Project Team [15] noted that a model assuming variable fracture aperture gave somewhat better fits to experimental data for non-sorbing tracer than the advection-dispersion model assuming constant fracture aperture.

6.3 Unresolved Issues

As mentioned above it is not clear from the calibration results whether hydrodynamic dispersion or channelling dispersion should be included in a model describing the experiments in this test case. The KTH Team [10] concluded that a distinction between the models cannot be made using experiments with a constant migration distance.

6.4 Proposals for Further Experiments

The Project Teams presented ideas of improving the design of future potential experiments of the type on which this case is based. One suggestion given by the PNL Team [16] was to increase the length of the core and thereby reduce the uncertainty associated with the estimated values of some of the parameters. The KTH Team [10] indicated that if an experiment could be designed in such a way that migration over different distances in the same fracture could be studied, it might be possible to distinguish between hydrodynamic dispersion and channelling dispersion.

It was also suggested by the PNL Team [16] that experiments should be performed with simultaneous injection of a non-sorbing and a sorbing tracer. This would make it possible to determine the flow parameters independently of the parameters determining the interactions of rock and tracer. Furthermore, the team suggested simultaneous injection of a diffusive tracer and a non-diffusive tracer such as large molecular weight lignosulfonates, to obtain independent information on matrix diffusion.

The KTH Project Team proposed tracer experiments using different flow rates to obtain more information about the mechanisms of matrix diffusion. The use of non-sorbing or weakly sorbing tracer in combination with low flow rates could give information on possible variations in the diffusion when the tracer reaches locations some distance away from the fracture surface.

Finally, the PNL Project Team [16] suggested that synthetic experiments should be carried out prior to the real experiments. This should be a cost effective way to study different experimental conditions in order to obtain a good design of the experiments.

6.5 Implications for Performance Assessment

As was stated in the Introduction Chapter, the temporal and spatial scales of laboratory experiments are much too small to give data on geometrical structures and scale-dependent parameters that are relevant for performance assessment. Laboratory experiments can, however, help to increase our understanding of transport processes and mechanisms, especially processes acting on a small scale. In particular this test case provides additional support for the inclusion of matrix diffusion and matrix sorption in models used in performance assessment of repositories in fractured rock.

References

1 INTRACOIN, Final Report Level 1, "Code Verification", SKI 84:3, September 1984, and Final Report Levels 2 and 3, "Model Validation and Uncertainty Analysis", SKI 86:2, Swedish Nuclear Power Inspectorate, Stockholm, May 1986.

2 The International HYDROCOIN Project, "Level 1: Code Verification", OECD/NEA Swedish Nuclear Power Inspectorate, 1988, and "Level 2: Model Validation", OECD/NEA Swedish Nuclear Power Inspectorate, 1990.

3 Geosphere Transport Model Validation - A Status Report, SKI 87:4, Swedish Nuclear Power Inspectorate, June 1987.

4 INTRAVAL Project Proposal, SKI 87:3, Swedish Nuclear Power Inspectorate, July 1987.

5 Eriksen T.E.,"Radionuclide Transport in a Single Fissure, A Laboratory Study of Am, Np, and Tc", KBS Technical Report, TR 83-01, SKB, Stockholm, Sweden, 1983.

6 Eriksen T.E.,"Radionuclide Transport in a Single Fissure, A Laboratory Study", KBS Technical Report, TR 84-01, SKB, Stockholm, Sweden, 1984.

7 Eriksen T.E.,"A Laboratory Study on Radionuclide Migration in Single Natural Granitic Fissures", Nuclear Technology, Vol.70, pp.261-267, 1985.

8 Eriksen T.E. and B. Locklund,"Radionuclide Sorption on Crushed and Intact Rock, Volume and Surface Effects", SKB Technical Report, TR 89-25, SKB, Stockholm, Sweden, 1989.

9 Neretnieks I., Eriksen T.E. and P. Tähtinen,"Tracer Movement in a Single Fissure in Granitic Rock: Some Experimental Results and their Interpretation", Water Resources Res., Vol.18(4), pp.849-858, 1982.

10 Moreno L., Neretnieks I. and T.E. Eriksen,"Analysis of Some Laboratory Tracer Runs In Natural Fissures", Water Resources Res., Vol. 21(7), pp. 951-958, 1985.

11 Carlsson L., Stejskal V. and T. Olsson,"Core-Logs of Borehole VI Down to 505 m. Part I", Stripa Project, IR 81-05, SKB, Stockholm, Sweden, 1981.

12 Carlsson L., Stejskal V.and T. Olsson,"Core-Logs of the Subhorizontal Boreholes N1 and E1", Stripa Project, IR 82-04, SKB, Stockholm, Sweden, 1982.

13 Carlsson L., Eggert T., Westlund B. and T. Olsson,"Core-Logs of the Vertical Borehole V2", Stripa Project, IR 82-05, SKB, Stockholm, Sweden, 1982.

14 Carlsson L. and T. Olsson,"Hydrogeological and Hydrogeochemical Investigations in Boreholes - Final Report", Stripa Project, TR 85-10, SKB, Stockholm, Sweden, 1985.

15 Kimura H., Munakata M, "Analysis of Tracer Movement in a Single Fracture in Granite Core (INTRAVAL case 2)", Journal of Nuclear Science and Technology, Japan (in press).

16 Aimo N.J.,"Analysis of One-Dimensional Transport in a Fracture with Matrix Diffusion using Parameter Estimation Techniques", Draft Project Team Report from Pacific Northwest Laboratory (PNL), September 1989.

17 Skagius K., Svedberg G, Neretnieks I, "A Study of Strontium and Cesium Sorption on Granite", Nucl. Techn., 59, p 302, 1982.

Appendix A

Test Case 2 Participants

The following project teams have participated in this test case:

The Royal Institute of Technology (KTH), Sweden
Project Team Leader: Ivars Neretnieks
Contributing author: Luis Moreno

Batelle Pacific Northwest Laboratories (PNL), USA
Project Team Leader: Nino Aimo
Contributing author: Nino Aimo

Japan Atomic Energy Research Institute (JAERI), Japan
Project Team Leader: Hideo Kimura
Contributing author: Hideo Kimura

OECD PUBLICATIONS, 2 rue André Pascal, 75775 PARIS CEDEX 16 - No. 78676 1992
PRINTED IN FRANCE

THE INTERNATIONAL INTRAVAL PROJECT

Phase 1 Test Cases

Intravel parties:
Agence Nationale pour la Gestion des Déchets Radioactifs (France), Atomic Energy of Canada Ltd. (Canada), Australian Nuclear Science and Technology Organisation (Australia), Bundesanstalt für Geowissenschaften und Rohstoffe/Bundesamt für Strahlenschutz (Germany), Commissariat à l'Energie Atomique/Institut de Protection et de Sûreté Nucléaire (France), Empresa Nacional de Residuos Radioactivos S.A. (Spain), Gesellschaft für Reaktorsicherheit (Germany), Gesellschaft für Strahlen- und Umweltforschung (Germany), Her Majesty's Inspectorate of Pollution (United Kingdom), Industrial Power Company Ltd. (Finland), Japan Atomic Energy Research Institute (Japan), Nationale Genossenschaft für die Lagerung Radioaktiver Abfälle (Switzerland), National Institute of Public Health and Environmental Hygiene (the Netherlands), National Radiological Protection Board (United Kingdom), Nuclear Safety Inspectorate (Switzerland), Power Reactor and Nuclear Fuel Development Corporation (Japan), Swedish Nuclear Fuel and Waste Management Co. (Sweden), Swedish Nuclear Power Inspectorate (Sweden), U.K. Nirex Ltd. (United Kingdom), U.S. Department of Energy (United States), U.S. Environmental Protection Agency (United States), U.S. Nuclear Regulatory Commission (United States).

Observers: International Atomic Energy Agency (IAEA), State of Nevada (United States).

Project Secretariat: Swedish Nuclear Power Inspectorate, Her Majesty's Inspectorate of Pollution/Harwell Laboratories, Kemakta Consultants Co., Organisation for Economic Co-operation and Development/Nuclear Energy Agency.

Copies of this report are available from:

The Swedish Nuclear Power Inspectorate (SKI)
Box 27106
S-102 52 Stockholm (Sweden)